

INTEGRATED USE OF TM IMAGE, DTM AND 3D VISUALIZATION IN GROUNDWATER STUDIES ON KARSTIFIED MARBLES

A. Dimadi^{a,*}, M. Tsakiri-Strati^b

^a Dept. Geotechnical Engineering, Aristotle University of Thessaloniki, GREECE, adimad@civil.auth.gr

^b Dept. Cadastre, Photogrammetry and Cartography, Aristotle University of Thessaloniki, GREECE, martsak@vergina.eng.auth.gr

Working Group VII/3

KEY WORDS: Geology, Resources, Integration, Interpretation, Navigation, Visualization, DTM, Landsat

ABSTRACT:

The purpose of this study was the evaluation of integrated use of landsat TM imagery, Digital Terrain Model (DTM) and 3D visualization for groundwater studies on karstified marbles. It was used a multispectral TM landsat imagery and a DTM that derived from the topographic map. The study area is a mountainous area of karstified marbles in Northern Greece. The faults control the hydraulic conductivity of the marbles, and their mapping is a very valuable means of identifying potential sites for groundwater exploitations. Applied image enhancement techniques were used, such as: principal components analysis, empirical and statistical procedures for color composite display of image, NDVI index and haze reduction in order to facilitate the detection of necessary criteria, (which are various geological and geomorphological factors), for the fault structures mapping. Draping the orthorectified image over the generated DEM in order to 3D visualization was applied. The supervised navigation on image 3D visualization was improved the image interpretation. The results obtained have been evaluated using both an existing geologic map of the area and a field investigation including: a) measurements of faults and definition of their nature, b) positions of springs, sinkholes, shallow holes, an axis cave with subterranean river and c) the results of boreholes. The applied methodology shows that a large number of fault structures were mapped, particularly in E-W direction and as a consequence a more completed net of faults was created. Further more the tension faults N0°-20°, N50°, N90°, and N120°-160° show a greater hydraulic conductivity and delineate potential sites for groundwater exploitations as the well yield data confirm this. The overall benefit of this methodology is the reduction of the risk of low yield wells.

1. INTRODUCTION

The use of satellite images is one of the technique that are available to hydrogeologists for locating and mapping linear faulted structures which can be faults and faulted zones (lineaments) (Sander et al., 1996). These secondary permeability features control the permeability of carbonate rocks those the primary porosity is usually extremely limited. Consequently the potential sites for productive water wells are located around the features with secondary permeability (Parizek, 1975; Larsson, 1977; Dinger, et al, 2002; Travaglia, et al 2003).

The advantage of the use of satellite images is that these cover big and sometimes inaccessible areas, under uniform conditions. Especially the capability of TM imagery to be analyzed for enhancing the visibility of lineaments, contribute to the effective study of lineaments on the earth surface.

This research presents a methodology of locating and mapping faults in the area of west Falakro mount (East Macedonia-Greece). This area is a rugged karstified carbonate mountainous terrain and forms a geomorphological natural dam between Drama basin and Kato Nevrokopi basin in the North. The study area covers parts of two topographical maps at scale 1:50,000 in UTM projection. These maps are used for the creation of the digital terrain model (DTM) and for receiving the control points for the orthorectification of the image.

The criteria of localization and mapping the lineaments are: a) the presence of vegetation, b) wetness, c) different slopes on both sides along the lineament and d) different geological formations on both sides (Meladiotis et al., 2001).

To facilitate the image optical interpretation for the lineaments localization, the spectral characteristics of the image bands were studied and the principal components transformation and vegetation index were applied, as the statistical or empirical procedures for image color display were applied (Yésou et al. 1993; Tsakiri, et al 2002; Tsakiri, et al 2003). Some of the aforementioned criteria could not be detected so we applied the supervised navigation on 3D visualization of DTM in combination with orthoimage to facilitate the localization and the mapping of the lineaments (Sarapirome, et al, 2003).

The hydrogeological importance of some particular fault systems can be examined through their combination with karst specific forms (sinkholes, shallowholes, caves), which usually are developed along faults. So these fault systems can have a secondary permeability and define probable general direction of groundwater flow (Kresic, 1995).

The lineaments coverage layer was overlain on the digitized topographic map (scale 1:50,000) for field checking. The field reconnaissance has offered the identification of many lineaments on the ground through their terrain features. The majority of the lineaments are tensional faults and the drilling

* Corresponding author.

potential sites are located in the vicinity of these faults, as the result of the three water wells on the foothill confirmed.

2. STUDY AREA AND DATA

In the frame of this work, it was used a multispectral image TM of Landsat 5 satellite, with a spatial resolution of 30 m and date of acquisition 22-05-1986. A subscene, covering about 20x18 km and including the karstified marbles, was extracted from this (Fig. 1). The statistical data on it are given in Table 1. For the ortho-rectification of the image a DTM was used that derived from two topographic maps at 1:50,000 scale and in UTM projection (Tsakiri-Strati et al, 2003).

Band	Min-Max	Mean	St. dev.
TM1	68-255	93.053	12.251
TM2	21-186	40.402	7.018
TM3	12-252	39.428	12.437
TM4	15-255	102.772	20.834
TM5	7-255	96.938	23.519
TM7	1-255	36.426	14.711

Table 1. Landsat TM image characteristics

Also geological map at the scale of 1:50.000 (Fig. 2) were used for the evaluation of the results of this investigation as well as with results from other studies (Meyer, 1968; Dimadi, 1988; Chagipanagis, 1991).

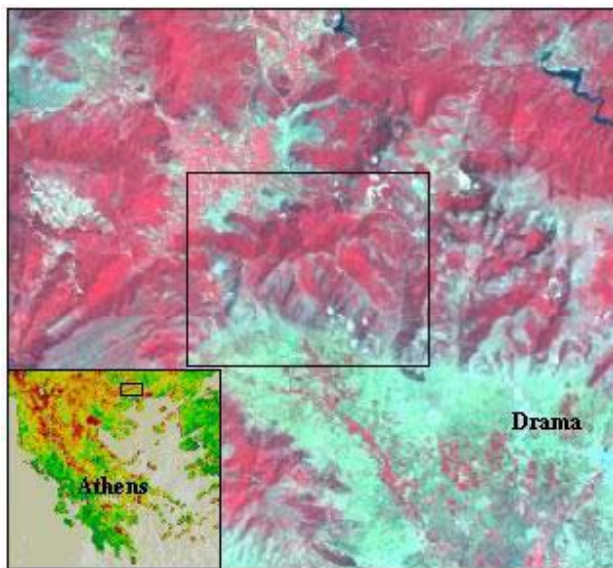


Figure 1. Landsat TM image over the study area. R=band4, G=band2 and B=band1.

3. GEOGRAPHICAL AND GEOLOGICAL SETTING

The study area corresponds to a mountainous terrain to the North of Drama (Greece) (Fig. 1). This is the Southwest part of Falakro mount (East Macedonia-Greece) with elevation between 123 m and 1736 m in the South and between 537 m and 1736 m in the North.

Southward is bordered by the plain of Drama and in the North by the Kato Nevrokopi basin (Polje). The area covers 103 km²

and 93% of it is marbles, the 3% dolomitic marbles and the 5% granodiorite. The vegetation of the area is some bushes in the Southern part and dense arboreous (beeches, pines) in the Northern part. The differentiation of vegetation in the region is owed only to the orientation of the surface and the height of rainfalls, so in the Northern part, marbles and granodiorite present the same vegetation in the same region.

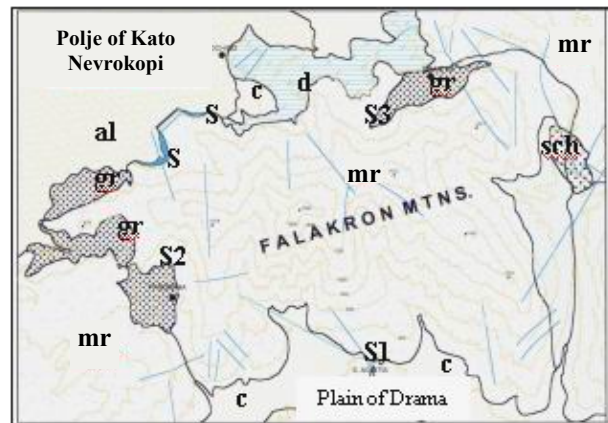


Figure 2. Geological map of the study area, 1:50,000 (IGME)
al: Sand, clay, c: conglomerates of marbles, mr: marbles,
d: dolomitic marbles, sch: schists, gr: granodiorite,
— Faults, — Geological boundary,
S1: spring Aggitis, S: sinkholes area

The drainage network has a dendritic pattern that is the same on the marbles and on the gneisses-schistes of the close region. This network on the marbles is old and was developed on the gneiss when they were above the marbles. The so-developed network was finally inherited on the marbles (Vavliakis et al. 1989; Dinter, 1994).

The area belongs to Geotectonic Zone of Rhodope and is a part of the West side of an anticlinal with axe N120°. It consists of marbles (Mesozoic) lying on the system gneiss-schist (Paleozoic). In the base, the marbles are white-gray and thin - platy, well bedded with muscovite on the bedding plane. On the top they are white and compact. Between the two sorts of marbles there are intercalations of dolomitic marbles. The granodiorite (Oligocene) penetrates all the aforementioned formations. During the Lower Oligocene ascending movements observed in the area, with the creation of shear zones (ENE-SWS) and in the Middle Miocene the area was folded with directions of folds axes N120°. The fractures related to the tectonic deformation before the Upper Miocene can not be distinguished from the fractures developed by a Upper-Miocene to present extensive brittle extensional deformation that mainly related to high-angle normal faults. The fault patterns include NE-NW (N0°- N20°), NW-SE (N50°), E-W (90°) and NW-SE (N120°-160°) trending faults (Chagipanagis, 1991).

The karst specific forms, sinkholes, are located between 800-1400 m along the crests and the shallowholes on the Northwest foot of the marbles at 540 m elevation.

The study area is a hydrogeological unit of karstified marbles and their alimentation originates directly by the rainfalls and indirectly by the streams and underground water of the polje of Kato Nevrokopi, in the area of shallowholes. The spring Aggitis (Fig. 2) located at an elevation of 123m, drains this

hydrogeological unit and the polje, with a mean annual discharge of 5m³/sec. The water is coming out from a large and imposing cave with a tube like shape (karstic conduit). This conduit connects the shallow holes and the spring. There are two other springs (Fig.2,7, S2, S3) at the elevation between 600-800m with mean annual discharge <1lit/sec (Dimadi, 1988).

4. DEM GENERATION AND ORTHO-RECTIFICATION OF THE IMAGE

For the creation of DTM, two topographic maps, at scale 1:50,000 and in UTM projection, were used (Tsakiri, et al., 2003). The image was orthorectified by using the generated DTM and 25 control points. The accuracy of the orthorectification was RMS=0,66 pixels.

5. SPECTRAL CONTENT INFORMATION

The six Landsats TM bands cover the visible region of spectrum, VIS (TM1, TM2 and TM3) the near infrared, NIR (TM4) and the middle infrared, MIR (TM5, TM7). In these regions of spectrum the rocks have different spectral characteristics. The MIR is characterized with high reflectance values for most of the rocks at the spectral range covered by TM5 and by strong absorption features for clays and micas at the TM7. Even if the TM bands do not allow precise discrimination of the mineral content in soils or rocks, it may be possible to detect some groups of minerals. The differences in the reflection can be due to the different lithological composition of bared soils that is created for example from the surface humidification of granite or micas chist slate. It is obvious that the soil on micas chist contains more micas and clays than soils on the granite with consequently the intense absorption (Yésou, et al. 1993; Tsakiri et al., 2003).

The comparison of the NIR and VIS provides the bare soils and vegetation discrimination. In the study area, the rocks are marbles, which are constituted from calcite that approaches the 90%, dolomitic limestone with calcite in 8% and dolomite in 92% and granodiorites mainly with feldspars (intense kaolinited) and quartz. As a result they have different spectral signatures. It is known that the spectral signatures allow the discrimination of the objects. The comparison of the bands in the near infrared and in the visible region provides the discrimination between the bare soil and the vegetation, as it is well known.

6. VISUALIZATION OF BAND COMBINATION

The six TM bands provide 20 possible combinations per three, for color display. To get an optimal color composite, the three bands used, must have the minimum redundancy that is to have the minimum correlation coefficient. Different ways exist to determinate of most optimal combination, which can be or empirical or statistical.

6.1 Empirical procedure

Three bands are selected based on their spectral characteristics. It is the most commonly used technique. This technique decreases the volume of possible combinations of bands. An optical study based on the spectral parameters and on the

radiometric contrast of different color composition allows the determination of best combinations in respect of information.

The combination TM5-4-2 allows the better perception of geological structures and the TM7-4-3 provides good discrimination between bare soil and vegetation. According to the international bibliography, the combinations TM7-5-1, TM7-5-4, TM4-3-1 and TM4-3-2 have poor contrast and do not facilitate the discrimination of rocks (Yésou, et al., 1993). These combinations for the imagery that was used in the present work, gave images suitable for interpretation that proves that the combinations are not submitted in rules but they depend on local characteristics (geology, geomorphology, vegetation). In this study were used combinations from empiric methodology depending on the area. For example, for the localization of the granodiorite was used the combination TM7-5-1. More frequency was used for the combination TM4-5-2 (Fig. 3).

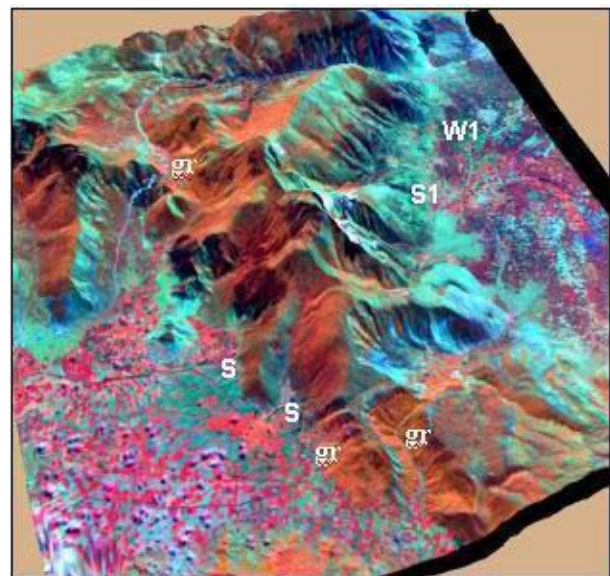


Figure 3. 3D Visualization of Landsat TM image, over the DEM, where: R=band4, G=band5 and B=band2. gr: granodiorite, S1: spring Aggitis, S: shallowholes area, W1: well

6.2 Statistical Procedure

The factor of most optimal index (Optimum Index Factor, OIF) is computed which is based on the variance and the correlation of bands. The Factor OIF is computed for each possible combination of three bands. The band combination, that has the bigger value in factor disposes, has the more information, and it is calculated according to the function (1). In Table 2 the OIF is presented for all the combinations of bands. In the third column is presented the degree where smallest corresponds in the bigger OIF and biggest in smallest.

$$OIF = \frac{\sum_{i=1}^3 \sigma_i}{\sum_{j=1}^3 |r_i r_j|} \quad (1)$$

where σ_i : the standard deviation of band i, i = 1, 2, 3
 $r_i r_j$: the correlation coefficient of bands i and j

$$NDVI = \frac{IR - R}{IR + R} \quad (2)$$

BAND COMBINATION	OIF	degree
TM1-2-3	11,13	20
TM1-2-4	55,26	10
TM1-2-5	17,26	15
TM1-2-7	12,79	18
TM1-3-4	86,90	5
TM1-3-5	19,86	12
TM1-3-7	14,79	17
TM1-4-5	90,27	3
TM1-4-7	105,22	1
TM1-5-7	20,43	11
TM2-3-4	59,65	9
TM2-3-5	16,85	16
TM2-3-7	12,53	19
TM2-4-5	59,91	8
TM2-4-7	67,95	7
TM2-5-7	17,29	14
TM3-4-5	87,73	4
TM3-4-7	101,13	2
TM3-5-7	19,39	13
TM4-5-7	70,25	6

Table 2. The OIF for all the combinations of bands is presented.

7. PRINCIPAL COMPONENTS ANALYSIS

The principal components were computed of the imagery. The PC₁, PC₂ and PC₃ contain the 98% of the image variance. The PC₁ gets more information from the near and middle infrared regions (TM4, TM5 and less from TM7). The PC₂ gets more from the near infrared (TM4) and the middle infrared region (TM5-7). Consequently it expresses the difference between the near and medium infrared region, it is presented as indicator of soil (contrary to the NDVI index). The PC₃ contains more information from the visible region (TM1, TM2, TM3), it can be said that it is a component with poor contrast.

The first three PC₁, PC₂, PC₃ new bands present the compression of spectral information of multispectral TM imagery Landsat. The three remainder bands, PC₄, PC₅ και PC₇ express less than 2% of the information. For this reason were used the three first components, (Tsakiri, et al 2003).

8. VEGETATION INDEX

It is known the importance of application of NDVI index in multispectral image of forest areas or of vegetation areas. The NDVI index is computed by the function:

Where: R = the band TM3 and IR = the band TM4

The image NDVI presents the vegetation cover.

9. INTERPRETATION

Lineaments (faults and faulted zones) mapping was carried out through supervised navigation on 3D visualization by the VirtualGIS programme of Imagine 8.5 (Fig. 4, 5) The use of different combinations (Tsakiri, et al, 2003) for the better color display of the imagery, was a consequence of the big changing of the elevations of the area and they facilitated the interpretation. The full collection of lineaments, as obtained from the above analyses, was compiled on a geological map at scale 50.000 (Fig. 7).

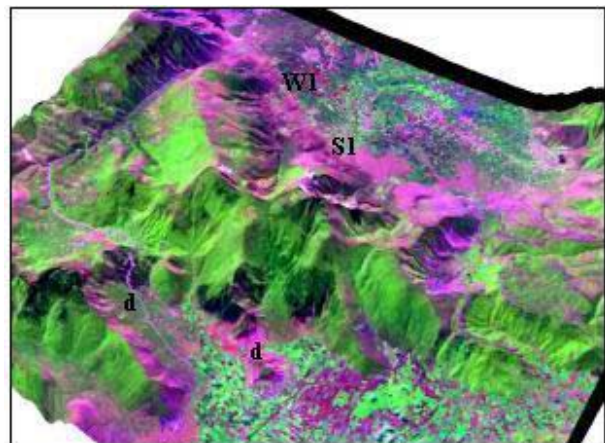


Figure 4. 3D Visualization of Landsat TM image, over the DEM, where: R=band7, G=band4 and B=band2.
d: dolomitic marbles, S1: spring Aggitis, WI: well

The faults and faulted zones are detectable mainly from pronounced vegetation anomalies, topographic effects or both. The tensional faults are easier to be recognized on the satellite image than the shear faults because they are open, wider easily weathered and with vegetation (Travaglia, et al 2003). In the present study the most of the faults were localized by vegetation anomalies, except the faults E-W, which localized by the supervised navigation (topographic effects-changing slopes). The human activities are very eliminated in the study area of marbles because of the elevation and the difficult access. Also the communities are located at the borders of the marbles.

The rose diagram (Fig.6a) presents the distribution of the directions of the lineaments (N20°, N50°, N90° and N120°-N160°) that were mapped (Fig. 7). These lineaments have the same directions with the faults (Fig.6,b) of the geological map except in the direction E-W (Fig. 2).

The interpretation key of satellite data is to locate karstic phenomena and compared with lineaments and that could give precious indications on which fractures allow higher circulation of water. The mapping of the sinkholes by the analysis of stereo

aerial photographs at scale 1:33,000 (Dimadi, 1988) shows that they are located along the faults of directions N55°, N80°, N110°, N125° and N140°.

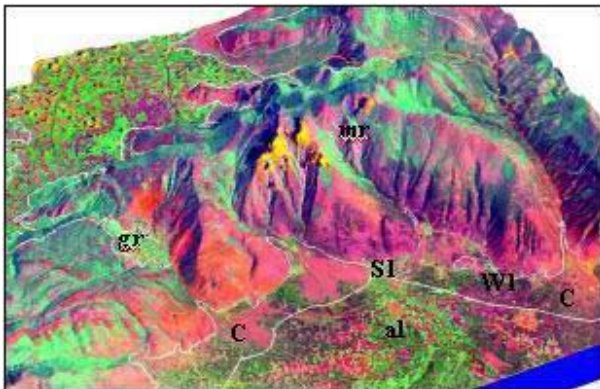


Figure 5. 3D Visualization of Landsat TM image, over the DEM, where: R=PC1, G=PC2 and B=PC3
al: sand, clay, c: conglomerates of marbles, mr: marbles, gr: granodiorite S1: spring Aggitis, W1: well

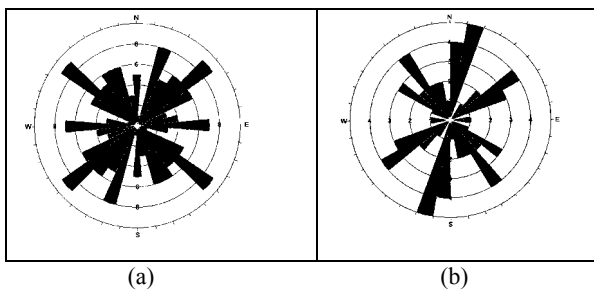


Figure 6. a) Rose diagram of the directions of the map lineaments (Fig. 7).

b) Rose diagram of the directions of the faults of geological map (Fig. 2).

The field checking identified the lineaments in the area of shallowholes (Fig. 7), and they are normal faults N10°, N50°, N90° N130°, N160° related with the development of the shallowholes. In the area of spring Aggitis a field checking identified the lineaments and they are normal faults also, with directions N90°, N100°, N125°, N140° and these directions are the same with the directions of the axe segments of the conduit. Also the spring S2 is located on the intersection of the lineaments N140° and N25° and the S3 on the intersection of the lineaments N45° and N160°.

Finally a potential drilling site was delimited on the foot of Falakro (Fig. 7) and three wells drilled: a) the well S1 on the intersection of the lineaments N115° and N50° with water yield 110m³/h, b) the well S2 on lineaments N115° with water yield 100m³/h and c) the well S3 in a distant of those two lineaments with water yield 15m³/h.

10. CONCLUSIONS

In this work the draping of the orthorectified image over the generated DEM in order to 3D visualization was applied. With the above process, the optical interpretation was improved as to

facilitate the locating and mapping of lineaments (faults, faulted zones). It was extremely supported by the supervised navigation so that many faults E-W were mapped although they were not represented by vegetation anomalies.

The hydrogeological research on karstified marbles (hard rocks) is trying to detect the faults that play a major role in karst ground water flow. These sorts of faults, in the study area, are in relation with the groundwater indicative data like as sinkholes, shallowholes, springs, conduit and they have directions: N20°, N50° N90° and N120°- 160°.

The field checking on the shallowholes area and around the spring S1, verified the results and that the faults are normal. The consequence was to delimit a potential site for drilling on southeast foot of marbles. Two wells were drilled near the intersection of two lineaments, N50° and N115°, and the third one in a distance from them.

The rate of the water yield of W1 and W2, for this area of Greece, is acceptable and it is a result that confirms the success of the mapping procedure using the satellite data.

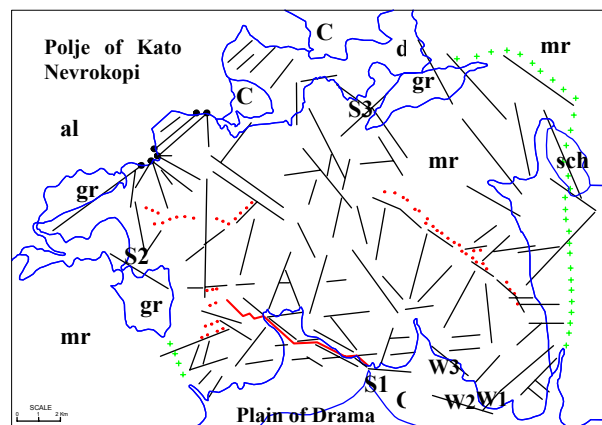


Figure 7. Geological map with the lineaments that mapped by using TM imagery

al: Sand , clay, c: conglomerates of marble, mr: marbles, d: dolomitic marbles, gr: granodiorite, sch: schists
— lineaments (fault,faulted zones), — Geological boundary, S1, S2, S3: springs, ●●● Sinkholes, ●: Shallowholes, — — — — — axe of the cave, ++++: boundary of Hydrogeological unit of marbles, W1, W2, W3: Wells Hydrogeological unit of marbles, W1, W2, W3: Wells

11. REFERENCES

- Dimadi, A., 1988. Comportement hydrogeologique des marbres de la bordure du Rhodope. Hydrogeologie du secteur sud-ouest du massif du Falakro-Macedoine Orientale, Greece. Ph. D. Univ. Grenoble I, France, pp. 214.
- Dinter, D., 1994. Tertiary Structural Evolution of the Southern Rhodope Province: A Fundamental Revision. *Proceedings of the 7th Congress*, Thessaloniki, May 1994. Bulletin of the Geological Society of Greece vol. XXX/1, pp.79-89, 1994.
- Dinger, J., Andrews, P., Wunsch, D., Dunno, G., 2002. Remote Sensing and field techniques to locate fracture zones for high-yield water wells in the Appalachian Plateau, Kentucky. *Proceedings of the National Ground Water Association*

Fractured-Rock Aquifer Conference, March 13-15, 2002, Denver, Colorado

Kresic, N., 1995. Remote Sensing of Tectonic Fabric Controlling Groundwater Flow in Dinaric Karst. *Remote Sensing of Environment*, vol. 53, pp. 85-90.

Larsson, L., 1977. Groundwater in hard rocks, International Seminar "Groundwater in Hard Rocks", Stockholm-Cagliari.

Meladiotis, I., M., Tranos and E., Tsolakopoulos, 2001. Localization and mapping of fault structures in the eastern part of the Askio Mountain (W. Macedonia, Greece) with the aid of digital satellite data. *Mining and Metallurgical Annals*, vol. 1-2/2001, pp. 19-34. (in Greek)

Meyer, W., 1968. Zur Altersstellung des Plutonismus im Sudteil der Rila-Rhodope-Masse (Nordgriechen-land). *Geol. et Palaeont.*, 2, pp. 173-192.

Parizek, R., 1975. On the nature and significance of fracture traces and lineaments on carbonated other terranes. *Proceeding of the US-Yugoslavia Symposium on the Karst Hydrology and Water Resources*, *Water Resources Publications*, Fort Collins, Colorado, USA.

Sander, P., M., M., Chesley, T., B., Minor, 1996. Groundwater assessment using Remote Sensing and GIS in a rural groundwater project in Ghana. *Hydrology Journal*, vol. 4, no. 3, pp. 40-49.

Sarapirome, S., A., Surinkum, P., Saksuthipong, 2003. Application of DEM Data to Geological Interpretation: Thong Pha Phum Area, Thailand.
Email: sunya@dmr.go.th

Travaglia, C., N., Dianelli, 2003. Groundwater Search by Remote Sensing: A Methodological Approach. FAO. Environment and Natural Resources Service Sustainable Development Department. ROME, pp. 34.

Tsakiri-Strati, M., A., Dimadi, 2003. *Integrated use of TM image of Landsat satellite and DTM for geological limits and fault structures localization*. From Stars to Earth and Culture, Aristotle University of Thessaloniki, Greece, pp. 113-120. (in Greek)

Tsakiri-Strati, M., B., Tsioukas and M., Papadopoulou, 2002. Fusion of PAN and MS images of IKONOS 2 Satellite. Evaluation of spatial accuracy and spectral quality of derived image: *Proceedings of the 6th National Geographic Congress of Hellenic Geographic Chamber*, Thessaloniki, in CD. (in Greek)

Vavliakis, E., N., Lambrinos, Th., Langalis, G., Syrides, 1989. The Polje of Kato Vrontou-Kato Nevrokopi the Rila-Rhodope massif. *GEOGRAPHICA RHODOPICA*, vol. 1. Kiment Ohridski University Press, Sofia, pp. 54-63.

Yésou, H., Y., Bensus and Rolet, 1993. Extraction of spectral information from Landsat TM data and merger with SPOT panchromatic imagery a contribution to the study of geological structures. *ISPRS Journal of Photogrammetry and Remote Sensing*, 48(5), pp. 23-36.

Chagipanagis, I., 1991. Geological structures of abroad area of mountain Falakro. National Techn. University of Athens, Dept. Mining Engineering and Metallurgy, Ph. D, pp. 179.